

The effect of power-drive level on the calibration of the bridge instrument for the measurement of the quartz stability

F. Sthal, S. Galliou, J. Imbaud, X. Vacheret,
P. Salzenstein, E. Rubiola

Frequency and Time Department, FEMTO-ST Institute
CNRS, ENSMM, UFC, UTBM
Besançon, France
fsthal@ens2m.fr

G. Cibieli

Microwave and Time-Frequency Department
CNES
Toulouse, France

Abstract— In this paper, it is shown that the amplitude-frequency effect, a well known phenomenon in quartz crystal resonator, questions the short-term stability results of quartz crystal resonators computed from phase noise measurement in passive interferometer systems. This equipment allows one to measure the inherent phase stability of quartz crystal resonators in a passive circuit without the noise usually associated with an active oscillator. The short-term stability of the resonator given by the Allan standard deviation is usually computed with the Leeson frequency. A new method to characterize the short-term stability of crystal resonators by a phase bridge system is given.

I. INTRODUCTION

High-stability quartz oscillators are needed in a number of space applications. Highest stabilities have been observed on 5 MHz and 10 MHz bulk acoustic-wave resonators [1]. Since 1975, researchers try to distinguish the resonator noise in the crystal oscillator by means of passive systems [2-5]. Some models have been tested in order to distinguish the resonator and the oscillator noises [6-8].

Carrier suppression techniques to characterize the inherent phase stability of ultra-stable quartz crystal resonator were demonstrated at the beginning of the 21st century [9-10]. Recently, an advanced version of this instrument has been implemented at FEMTO-ST, in collaboration with the CNES and with the major European manufacturers of high stability resonators [11-14].

The instrument is based on the synchronous detection of the noise sideband after suppressing the carrier by vector sum of an equal and opposite reference signal. The detected noise is measured with a fast Fourier transform analyzer. Since a reference source of noise lower than that of the resonators under test is not available, we use a symmetric scheme that compares two equal resonators, rejecting the noise of the source.

The usual way to calibrate the system is to inject in one arm of the bridge a sideband of known frequency and amplitude. The instrument gain is calculated from the amplitude of the detected signal. Then, the short-term stability of the resonator is deduced from the resonator filter effect. We observed that this practice may be incorrect when the drive power level of the resonator is increased. The reason is that the non-linearity, inherent in the quartz lattice, warps the shape of the frequency response, breaking the symmetry between upper and lower sidebands. Consequently, the quartz is no longer described by a 2nd-order linear differential equation. This phenomenon is definitely not negligible at the power levels of interest. The measurement of a few batches from different manufacturers reveals inconsistencies correlated to power. After reviewing the state of the art, this article proposes a new calibration method.

II. REVIEW OF THE MEASUREMENT BENCH

A. Bench Principle

The bench principle uses carrier suppression technique [9-10]. The general idea of this passive method (Fig. 1) consists in reducing the noise of the source as much as possible.

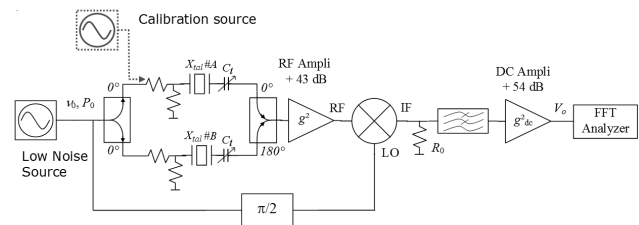


Figure 1. Principle of the measurement bench.

Indeed, when resonators exhibit a very weak noise, the noise of the source is always higher than that of the quartz crystal resonator. Thus, the direct feeding of the driving source

signal through only one resonator does not permit to extract the resonator noise from the output resulting noise. On the other hand, the source signal can be subtracted when passing through two identical arms equipped with identical resonators (the devices under tests: DUT). Then the contribution of the source is cancelled while inner noise of both resonators is preserved because one resonator noise is different from the other one. When the carrier suppression is achieved (less than -75 dBc is acceptable), the resulting signal only made up noise from both resonators, is strongly amplified and mixed with the source signal to be shifted down to the low frequency domain and processed by the spectrum analyzer. In such a way, noise to be measured from both resonators can be brought up at a higher level than the driving source noise. Moreover, the noise floor of the bench can be measured with resistors substituted for crystal resonators. Fig. 2 shows the measurement system.

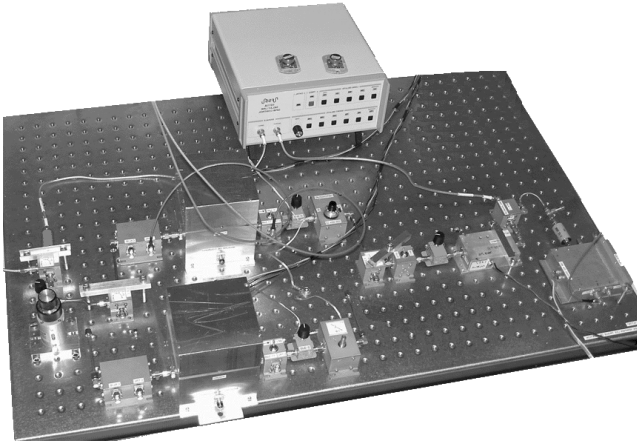


Figure 2. Measurement bench of resonator phase noise.

Calibration of the measurement system is obtained by injecting a known side band on one of the arms of the bridge. The noise of the DUT, as seen on the fast Fourier transform analyzer, is corrected using the calibration factor determined with the side band.

The input power of the bench comes from a synthesizer referenced to an ultra-stable OCXO. It is used at a typical power level. The power adjustment in the bench is realized by step attenuators. The crystal dissipated power can be moved from a few μW to approximately 200 μW . Each resonator is driven in the bench arm through an input resistance network matched to 50 Ω impedance. This network is composed of two resistances and depends on the motional resistance of the resonator. They are welded near the resonator and inside the oven. The resonator is associated with a tuning capacitor to get the resonance of the resonator at the source frequency. But, in our configuration, the frequency tuning can be done also with the synthesizer frequency at a constant tuning capacitor. The tuning method can be chosen according to the observed phenomenon. To get 200 μW inside the resonator, the input power of the bench should be sufficient to take into account the insertion loss.

The noise floor of the bench has been studied according to the output power of the driving synthesizer. DUTs are resistors. The DUT dissipated power is maintained constant by

tuning the input attenuator of the bench. Fig. 3 shows the one-sided power spectral density of the phase fluctuations $\mathcal{L}(f)$ versus the Fourier frequency with the synthesizer output power as a parameter. Measures are given at 10 MHz.

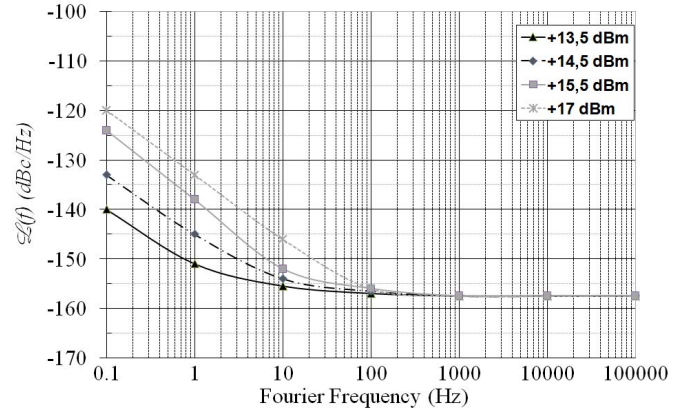


Figure 3. Noise floor of the measurement system according to the input power.

Below 100 Hz, the noise floor goes up when the output power of the synthesizer increases. The synthesizer output power must be under 15.5 dBm to get a floor below -140 dBc/Hz at an offset frequency of 1 Hz. The insertion loss between the bench input and the resonator input has a minimum value of -8.2 dB. Thus, with a synthesizer output power of +15.5 dBm, the maximum input power into the resonator is 7.3 dBm. If the motional resistance of the resonator is around 50 Ω , the maximum of the crystal dissipated power is about 215 μW .

B. Classical determination of the resonator short-term stability

Classically, the floor of the short-term stability of the resonator is given by the Allan standard deviation, $\sigma_y(\tau)$ [3]. The Allan deviation calculated this way represents the Allan deviation of an oscillator containing the tested resonator in which the only source of flicker frequency noise is the tested resonator. In the case of Flicker frequency noise, relation between the Allan standard deviation and the power spectral density (PSD) of relative frequency fluctuations $S_y(f)$, is given by:

$$\sigma_{y_floor} = \sqrt{2 \ln 2 S_y(1\text{Hz})} \quad (1)$$

$S_y(f)$ is given by the PSD of the phase fluctuations, $S_\phi(1\text{Hz})$, and the half bandwidth also called the Leeson frequency F_L :

$$S_y(1\text{Hz}) = \left[\frac{F_L}{f_{res.}} \right]^2 S_\phi(1\text{Hz}) \quad (2)$$

with $f_{res.}$ the resonant frequency of the resonator.

The Leeson frequency is obtained with the asymptotic crossing of the resonator filtering effect (Fig. 4). The resonator

is considered as a low pass filter. The transfer function of the resonator is given by the injection of a white noise source at the resonator input.

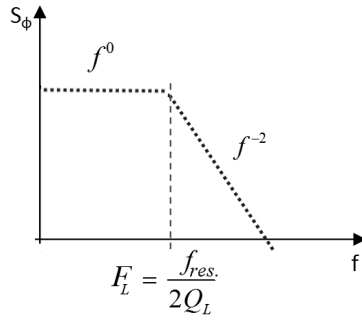


Figure 4. Transfer function of the resonator measured with white noise. Q_L is the loaded quality factor of the resonator.

The relationship between the Leeson frequency and the loaded quality factor Q_L of the resonator is given by:

$$F_L = \frac{f_{res.}}{2Q_L} \quad (3)$$

As an example, the measured $\mathcal{L}(f)$ of both 5 MHz resonators is shown in Fig. 5. The Leeson frequency could be determined by $\mathcal{L}(f)$ curve at the intersection of the f^{-1} and f^{-3} asymptotes but the precision is better by means of resonator transfer function.

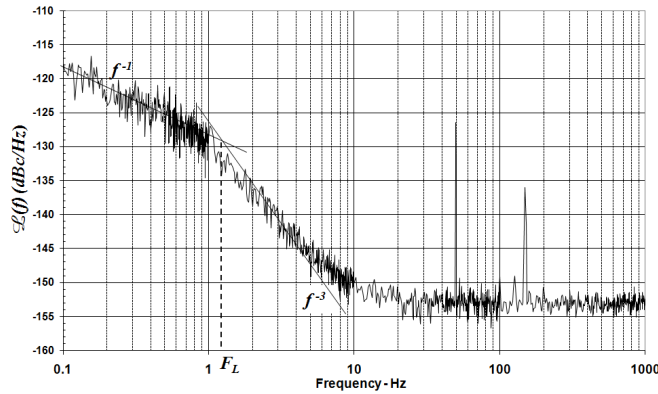


Figure 5. Typical $\mathcal{L}(f)$ of 5 MHz SC-cut resonators.

In this case, the drive power level of the resonator is 20 μ W. F_L is about 1.3 Hz and the floor of the short-term stability σ_{y_floor} is equal to $1 \cdot 10^{-13}$.

III. RESONATOR DRIVE POWER INFLUENCE

A. Resonator amplitude frequency effect

The measured resonators are 5 MHz SC-cut crystals. Drive power level P_{Xtal} of the resonators can be varied from 20 μ W to 200 μ W. The variation of the Leeson frequency is shown in Fig. 6 for these both extreme cases. The Leeson frequency is approximately divided by two.

Consequently to the $\mathcal{L}(f)$ measurements, table 1 sums up the σ_{y_floor} obtained with the method described before. The

short-term stability of the resonator seems to be really better at 200 μ W than at 20 μ W. Unfortunately, a simple calculus shows that the method to obtain σ_{y_floor} is not realistic. Typically, a 5 MHz ultra-stable resonator exhibits an unloaded quality factor of about $2.5 \cdot 10^6$. By means of (3), the loaded quality factor goes from $1.9 \cdot 10^6$ to $4 \cdot 10^6$. The loaded Q could become higher than the unloaded Q for resonator dissipated power up to 100 μ W.

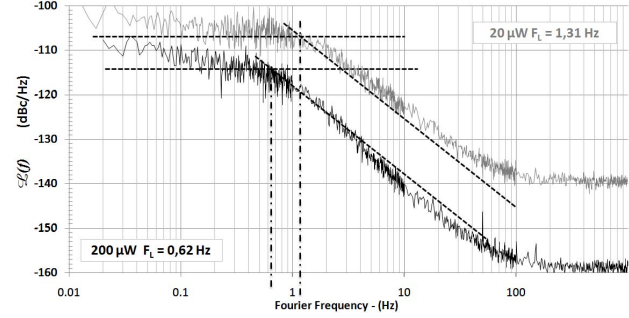


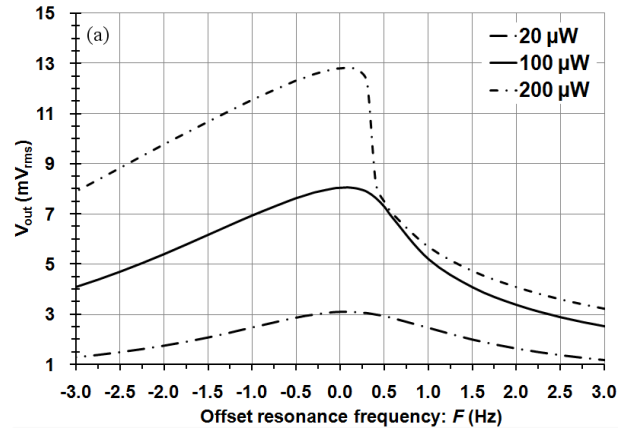
Figure 6. 5 MHz SC-cut Resonator transfer functions at 20 μ W and 200 μ W.

TABLE I. σ_{y_floor} ACCORDING TO THE RESONATOR DISSIPATED POWER, P_{XTAL} . RESONATORS ARE 5 MHz SC-CUT QUARTZ CRYSTALS

P_{Xtal} (μ W)	$\mathcal{L}(1 \text{ Hz})$ (dBc/Hz)	F_L (Hz)	σ_{y_floor}	Q_L (10^6)
20	-121.49	1.31	$3.67 \cdot 10^{-13}$	1.9
60	-126.74	0.96	$1.47 \cdot 10^{-13}$	2.6
100	-128.53	0.79	$9.84 \cdot 10^{-14}$	3.1
150	-129.81	0.68	$7.31 \cdot 10^{-14}$	3.7
200	-129.96	0.62	$6.55 \cdot 10^{-14}$	4

In the noise measurement bench, the transfer function of the resonator is obtained at Fourier frequency. Thus, the noise spectrum is fold up around the carrier frequency. To analyze the phenomenon, function transfer of the resonator must be observed at the carrier frequency with a network analyzer. Resonators have been measured in their impedance matching (PI) network by means of 4195A network analyzer.

Fig. 7 shows the transfer function of the resonator inserted in the PI network for different dissipated powers. The gain and the phase of the transfer function are given for three resonator dissipated powers.



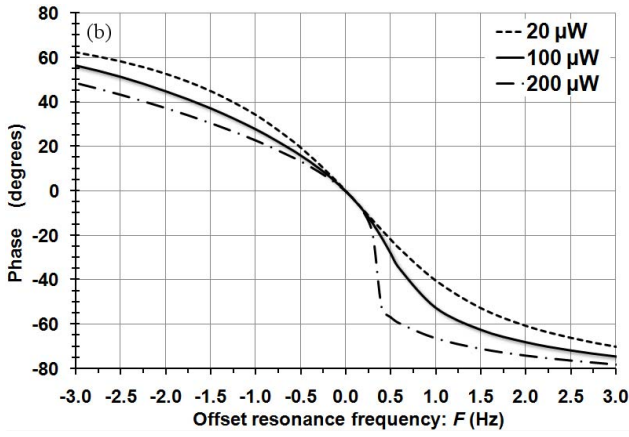


Figure 7. 5 MHz SC-cut resonator transfer functions obtained around its resonant frequency and according to P_{Xtal} .

The well known amplitude-frequency effect of the quartz crystal is clearly shown. The low pass filter effect of the resonator can be characterized by the 3 dB or $\pm 45^\circ$ bandwidth defined by:

$$\Delta F = \left| F_{-}(V_{out\ max} / \sqrt{2}) - F_{+}(V_{out\ max} / \sqrt{2}) \right| = 2F_L$$

or

$$\Delta F = |F_{-}(45^\circ) - F_{+}(-45^\circ)| = 2F_L$$

Where $F_{-}(V_{out\ max}/\sqrt{2})$ and $F_{+}(V_{out\ max}/\sqrt{2})$ are the frequencies of the transfer function which correspond with the amplitude equal to $V_{out\ max}/\sqrt{2}$. $F_{-}(45^\circ)$ and $F_{+}(-45^\circ)$ are the frequencies of the transfer function which correspond with a phase equal to $\pm 45^\circ$.

TABLE II. 3dB BANDWIDTH AND $\pm 45^\circ$ BANDWIDTH MEASURED AROUND THE RESONANCE FREQUENCY OF THE RESONATOR.

P_{Xtal} (μW)	$f_{res.}(V_{out\ max})$ (Hz)	3dB bandwidth			$\pm 45^\circ$ bandwidth		
		F_{-} (Hz)	F_{+} (Hz)	F_L (Hz)	$F_{-}(45^\circ)$ (Hz)	$F_{+}(-45^\circ)$ (Hz)	F_L (Hz)
20	4 999 999.10	-1.44	1.22	1.33	-1.5	1.17	1.33
60	4 999 999.43	-1.59	1.05	1.32			
100	4 999 999.79	-1.79	0.88	1.33	-2.5	0.81	1.65
150	5 000 000.25	-2.03	0.65	1.34			
200	5 000 000.66	-2.23	0.45	1.34	2.63	0.37	1.5

In the measurement system of the resonator noise, the spectrum folding explains that the positive half bandwidth F_{+} corresponds with the Leeson frequency measured by the white noise injected in the resonator (Fig. 8). This frequency does not represent the real value of the loaded quality factor of the

resonator. Thus, the great improvement of the short-term stability will be not seen in oscillator stability.

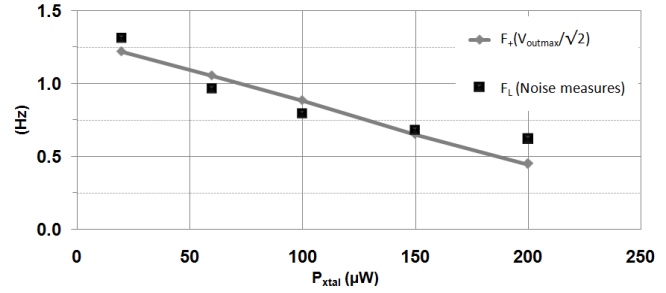


Figure 8. Comparison of Leeson frequency obtained with the classical way using the source noise injection and the positive half bandwidth obtained with the network analyzer around the resonant frequency of the resonator.

The classical calculus of the short-term stability must be done carefully with the drive level power of the resonator and its amplitude frequency effect.

B. New computation method

The previous method to compute the short-term stability by means of filter effect remains available for low power drive level. Therefore, Fig. 7b shows that the phase of the transfer function is not really affected by the drive power around the null phase. These curves are used in the conversion of the flicker frequency noise of the resonator into the measured phase noise. The Leeson frequency can be defined by the inverse of the slope of the relationship between $S_y(f)$ and $S_\phi(f)$ as the following expressions:

$$S_y(f) = \frac{1}{\left[f_{res.} \frac{d\phi}{df} \right]^2} S_\phi(f) \text{ then } F_L = \frac{1}{\left. \frac{\Delta\phi}{\Delta f} \right|_{\pm 2^\circ}} \quad (5)$$

Where $f_{res.}$ is the resonant frequency of the resonator. $\frac{d\phi}{df}$

is the derivative of the phase according to the frequency.

We chose to compute the slope between $\pm 2^\circ$ (Fig. 9). In this case, the linear hypothesis of the Leeson model is preserved. The measurement of this slope should be done in the same context as in the noise measurement. With this new method, the aberrant computation of the short-term stability and the loaded Q factor is not possible.

Table 3 shows a comparison of the short-term stability of the resonator. The noise source results are compared with the bandwidth methods of the filter effect and with our slope method. Better results are given with the slope method.

TABLE III. COMPARISON OF THE SHORT-TERM STABILITY CALCULUS IN THE WORST CASE WITH $P_{Xtal} = 200 \mu W$.

$\mathcal{L}(1\text{Hz})$ (dBc/Hz) -129.96	Slope ($\pm 2^\circ$)	Bandwidth ($\pm 45^\circ$)	Bandwidth (3 dB)	Noise source
F_L (Hz)	1.55	1.5	1.34	0.62
$\sigma_{y\ floor}$	$1.64 \cdot 10^{-13}$	$1.55 \cdot 10^{-13}$	$1.43 \cdot 10^{-13}$	$6.55 \cdot 10^{-14}$
Q_L	1 612 903	1 700 680	1 851 852	4 032 258
Q_L/Q_X	63 %	66 %	72 %	157 %

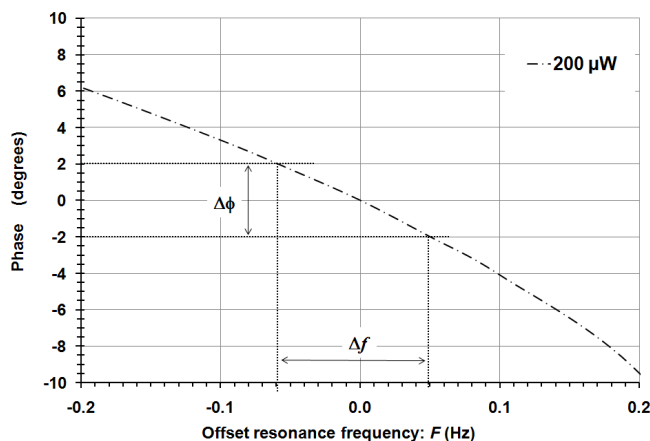


Figure 9. Phase-frequency relationship of the typical 5 MHz resonator. The slope of the curve is computed with $\pm 2^\circ$ for the critical case at $200 \mu\text{W}$.

IV. CONCLUSION

Passive measurement system of resonator phase noise has been reviewed. Several batches of different manufacturers have been tested. Particularly, measurements revealed that the short-term stability of the resonators observed according to the dissipated power could be unregular. This observation has been correlated to the amplitude-frequency effect, a well known phenomenon in quartz crystal resonator. These investigations have then led to reconsider the calibration method of the kind of measurement systems. A new method to compute the short-term stability of quartz crystal resonators is implemented.

REFERENCES

- [1] J. Chauvin, P. Weber, J.P. Aubry, F. Lefebvre, F. Sthal, X. Vacheret, "A new generation of very high stability BVA oscillators," Proc. Joint Meeting IEEE Ann. Freq. Cont. Symp. and European Frequency and Time Forum, Genova, Switzerland, June 2007, pp. 1261-1268.
- [2] F. L. Walls and A. E. Wainwright, "Measurement of the short-term stability of quartz crystal resonators and the implications for crystal oscillator design and applications," IEEE Trans. Instrum. Meas., vol. IM-24, pp. 15-20, Mar. 1975.
- [3] J. J. Gagnepain, "Fundamental noise studies of quartz crystal resonators," Proc. 30th Annu. Freq. Contr. Symp., Atlantic City (printed by Electronic Industries Association, Washington, DC), June 1976, pp. 84-91.
- [4] F. L. Walls, P. H. Handel, R. Besson and J. J. Gagnepain, "A new model of 1/f noise in BAW quartz resonators," Proc. 46th Annu. Freq. Contr. Symp., Hershey, PA (printed by IEEE, Piscataway, NJ), May 1992, pp. 327-333.
- [5] T. E. Parker and D. Andres, "1/f noise in surface acoustic wave (SAW) resonators," Proc. 48th Annu. Freq. Contr. Symp., Boston (printed by IEEE, Piscataway, NJ), June 1994, pp. 530-538.
- [6] S. Galliou, F. Sthal, M. Mourey, "New phase noise model for quartz crystal oscillators: Application to the Clapp Oscillator," IEEE Transactions on Ultrasonics, Ferroelectrics and Frequency Control, vol. 50, no. 11, November, pp. 1422-1426, 2003.
- [7] F. Sthal, S. Galliou, N. Gufflet, M. Mourey, "Predicting phase noise in crystal oscillators," IEEE Transactions on Ultrasonics, Ferroelectrics and Frequency Control, vol. 52, no. 1, January, pp. 27-31, 2005.
- [8] E. Rubiola, V. Giordano, "On the 1/f frequency noise in ultra-stable quartz oscillators" IEEE Transactions on Ultrasonics, Ferroelectrics and Frequency Control, vol. 54, no. 1, January, pp. 15-22, 2007.
- [9] E. Rubiola, J. Gros Lambert, M. Brunet and V. Giordano, "Flicker noise measurement of HF quartz resonators," IEEE Trans. Ultrason. Ferroelec. Freq. Contr., vol. 47, pp. 361-368, 2000.
- [10] F. Sthal, M. Mourey, F. Marionnet and W.F. Walls, "Phase noise measurements of 10 MHz BVA quartz crystal resonator," IEEE Trans. Ultrason. Ferroelec. Freq. Contr., vol. 47, p. 369-373, 2000.
- [11] S. Galliou, F. Sthal, X. Vacheret, R. Brendel, P. Salzenstein, E. Rubiola and G. Cibieli, "A program to analyze the origin of noise in ultra-stable quartz resonators," Proc. Joint Meeting IEEE Ann. Freq. Cont. Symp. and European Frequency and Time Forum, Genova, Switzerland, 29 May-1 June, pp. 1176-1181, 2007.
- [12] F. Sthal, X. Vacheret, P. Salzenstein, S. Galliou, E. Rubiola and G. Cibieli, "Advanced bridge instrument for the measurement of the phase noise and of the short-term frequency stability of ultra-stable quartz resonators," Proc. Joint Meeting IEEE Ann. Freq. Cont. Symp. and European Frequency and Time Forum, Genova, Switzerland, 29 May-1 June, pp. 254-260, 2007.
- [13] F. Sthal, S. Galliou, P. Abbe, X. Vacheret, G. Cibieli, "New ultra stable crystal ovens and simple characterisation," Electronics Letters, vol. 43, no. 16, 2nd August, pp. 900-901, 2007.
- [14] F. Sthal, S. Galliou, X. Vacheret, R. Brendel, P. Salzenstein, E. Rubiola and G. Cibieli "Analysis of noise origin in ultra stable resonators: preliminary results," Proc. 20th European Frequency and Time Forum, Toulouse, France, 25-27 April, FPE-0057.pdf, 2008.